Evaluation of Uncertainty in Damage Induced by Cardiac Cryoablation for the Treatment of Arrhythmias

Davi L F Rocha, Ruy F Reis

Universidade Federal de Juiz de Fora, Juiz de Fora/MG, Brazil

Abstract

In 2021, cardiovascular diseases accounted for 19.2 million deaths worldwide. Cryoablation has become an effective therapy for arrhythmias, particularly atrial fibrillation; however, its success depends on precise lesion formation, which is influenced by biological variability and procedural accuracy. This work presents a mathematical model of the cardiac cryoablation process with uncertainty quantification, utilizing Monte Carlo simulations to assess the impact of various conditions on tissue damage. Results show that freeze–thaw cycles and the duration of the thawing phase impact lesion extent. The proposed framework supports the analysis and optimization of ablation protocols, contributing to safer and more effective treatments of cardiac arrhythmias.

1. Introduction

Cardiac arrhythmias, particularly atrial fibrillation (AF), affect approximately 46.3 million people globally [1]. Cryoablation is a minimally invasive therapy that applies extreme cooling to myocardial tissue to produce controlled lesions [2]. Mathematical modeling and simulations of cryoablation allow the study of heat transfer, phase change, and tissue response, supporting improvements in the safety and efficacy of arrhythmia treatments.

Catheter ablation has become a standard treatment for cardiac arrhythmias such as AF, supraventricular tachycardias, and ventricular tachycardia [3]. Radiofrequency (RF) ablation is widely used; however, its reliance on high temperatures ($\geq 50^{\circ}$C) may lead to complications such as carbonization and tissue desiccation if not properly controlled [4]. Computational models of RF ablation have highlighted the importance of considering tissue properties such as density (ρ), specific heat (c), thermal conductivity (k), and electrical conductivity (σ) to understand lesion formation better [5].

Cryothermal ablation (cryoablation) has emerged as an alternative method, producing lesions through controlled freezing rather than heating. Meta-analyses have shown similar efficacy to RF with a favorable safety profile, and its clinical use has been steadily increasing [6]. In this context, mathematical modeling of cryoablation is crucial for describing heat transfer, phase-change phenomena, and thermal damage, providing insights into lesion geometry and supporting the optimization of treatment strategies for arrhythmias [7, 8].

The Pennes bioheat equation is widely employed to model heat transfer in living tissues and has been extensively applied in the context of cryoablation [2, 9, 10]. This formulation accounts for thermal conduction, metabolic heat generation, and blood perfusion, enabling a simplified yet effective description of the complex thermal interactions within the myocardium. When extended to incorporate temperature-dependent thermal properties and phase-change effects, the Pennes model provides a practical framework to simulate tissue cooling, ice formation, and lesion growth during cryosurgery, supporting both experimental interpretation and treatment planning [9]. For solving the mathematical model, we employ a Forward Time Centered Space (FTCS) scheme to compute the numerical solution, considering a heterogeneous medium [11].

We organise this paper as follows. Section 2 describes the bioheat model, numerical approximation, and the uncertainty quantification. The results are presented in section 3 and discussed in section 4. Finally, section 5 presents the conclusions and plans for future work.

2. Methods

2.1. Mathematical Model

The Pennes bioheat equation describes the heat transfer in living tissues:

$$\rho c \frac{\partial T}{\partial t} = \nabla \cdot (k \nabla T) + \omega_b \rho_b c_b (T_a - T) + Q_m, \quad (1)$$

where T is the tissue temperature and $T_a = 37^{\circ}$C the arterial blood temperature. The volumetric heat capacity ρc and thermal conductivity k vary with temperature to represent liquid ($T > 0^{\circ}$C), solid ($T < -10^{\circ}$C), and phase-change states ($-10^{\circ}\text{C} \leq T \leq 0^{\circ}$C). The perfusion term accounts for heat exchange with blood through ω_b, ρ_b, and

c_b, while Q_m represents metabolic heat generation. The complete problem, with boundary and initial conditions, is formulated as:

$$\begin{cases} \rho c \dfrac{\partial T}{\partial t} = \nabla \cdot k \nabla T + \omega_b \rho_b c_b (T_a - T) + Q_m & \text{in } \Omega \times I, \\ k \nabla T \cdot \vec{n} = 0 & \text{in } \partial\Omega \times I, \\ T(\cdot, 0) = 37.0 & \text{in } \Omega, \end{cases} \tag{2}$$

where $\Omega \subset \mathbb{R}^2$ represents the spatial domain, $I \subset \mathbb{R}^+$ denotes the time domain, and $T : \Omega \times I \to \mathbb{R}^+$ is the tissue temperature field.

2.2. Numerical Scheme

The finite difference method (FDM) was applied to solve Eq. (2) for the bioheat transfer problem. The simulation domain is a heterogeneous medium within a closed domain Ω, discretized into a uniform spatial grid with a spacing of h and a time grid with a step size of h_t. We discretize the governing equation using a FTCS scheme [11]. So, the explicit FDM formulation becomes:

$$\begin{aligned} T_{i,j}^{n+1} = T_{i,j}^{n} + \frac{\Delta t}{\rho c} \Big(& \nabla_h \cdot \left(k \nabla_h T^{\,n} \right) \\ & + \rho_b c_b \omega_b \left(T_a - T_{i,j}^{n} \right) + Q_m \Big), \end{aligned} \tag{3}$$

where

$$\begin{aligned} \nabla_h \cdot (k \nabla_h T^n) = \frac{1}{h^2} \Big[& k_{i+\frac{1}{2},j} \left(T_{i+1,j}^n - T_{i,j}^n \right) - \\ k_{i-\frac{1}{2},j} \left(T_{i,j}^n - T_{i-1,j}^n \right) & + k_{i,j+\frac{1}{2}} \left(T_{i,j+1}^n - T_{i,j}^n \right) - \\ & k_{i,j-\frac{1}{2}} \left(T_{i,j}^n - T_{i,j-1}^n \right) \Big]. \end{aligned} \tag{4}$$

This scheme has linear convergence, $O(h_t)$, in time and quadratic convergence, $O(h^2)$, in space. Within the FDM framework, thermal conductivity k is evaluated at cell interfaces using the harmonic mean, *e.g.*, $k_{i+1/2,j,k} \approx 2k_{i,j,k}k_{i+1,j,k}/(k_{i,j,k} + k_{i+1,j,k})$, to ensure flux continuity in heterogeneous medium. The stability condition from [12] is adopted to determine the time step h_t.

2.3. Thermal Damage

Thermal damage may occur either instantly, when the temperature drops below the cryogenic necrosis threshold $T_{nc} = -50°\text{C}$, or progressively, if the tissue remains below the cryogenic damage threshold $T_{dc} = -20°\text{C}$ for a sufficient period ($t_{dc} = 60\,\text{s}$) [10]. We evaluate the extent of injury by a destruction index $\beta_d \in [0, 1]$, where 0 indicates undamaged tissue and 1 corresponds to complete necrosis. For each cell, α is computed as:

$$\alpha = \begin{cases} 1, & \text{if } T \le T_{nc}, \\ \dfrac{1}{t_{dc}} \displaystyle\int_0^t (T < T_{dc})\, dt, & \text{if } T \le T_{dc}. \end{cases} \tag{5}$$

The destruction index is defined as $\beta_d = \min(1, \alpha)$. The integral in Eq. (5) was evaluated numerically using the rectangle rule, and the percentage of damaged tissue was derived from the count of cells where $\beta_d = 1.0$.

2.4. Uncertainty Quantification

The computational model allows the evaluation of how different freezing and thawing durations influence temperature evolution and tissue damage during cryoablation. In our study, after a fixed freezing period of $150s$, the effects of varying thawing durations were examined using Monte Carlo simulations. This method repeatedly samples from a random variable, specifically the thawing duration, to evaluate the effect of uncertainty on the outcome. So, we model the thawing phase using the following uniform distribution:

$$X \sim \mathcal{U}(5, 20), \tag{6}$$

where X is a random variable that represents the thawing duration. The range for the thawing duration is based on Handler [2].

3. Numerical Experiments

3.1. Computational Environment

We developed a numerical solver and implemented the Monte Carlo algorithm in C++, compiled with `gcc` 12.6 using the `-Ofast` flag. Parallel processing was enabled through OpenMP, and simulations were performed on an Intel®Core™ i7-10700 CPU (8 physical cores, 16 threads, 2.90 GHz) under Linux. Post-processing was carried out in Python with `Matplotlib`.

3.2. Simulation Scenario

To model cryoablation in the short-axis geometry (Fig. 1), temperature-dependent properties of tissue and blood were considered (Table 1). Thermal conductivity, specific heat, and fusion enthalpy were incorporated into the phase-transition range between $T_s = -10°\text{C}$ and $T_l = 0°\text{C}$, allowing a linear increase of ice content from 0% to 100% [9].

The temperature of the cryoprobe was modeled using a time-dependent Dirichlet condition. At each time step, the

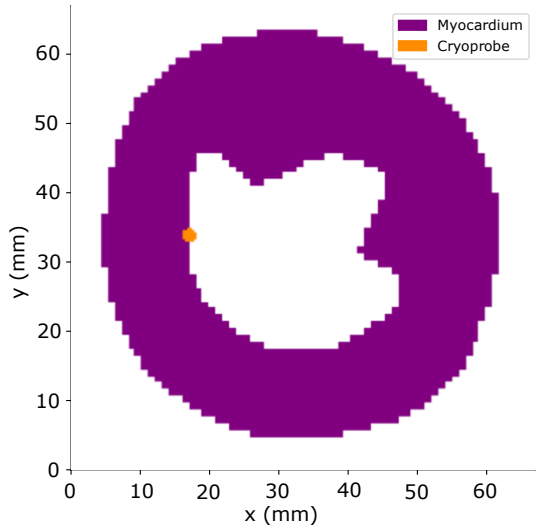

Figure 1. Short-axis ventricular domain discretized on a 200×200 grid points.

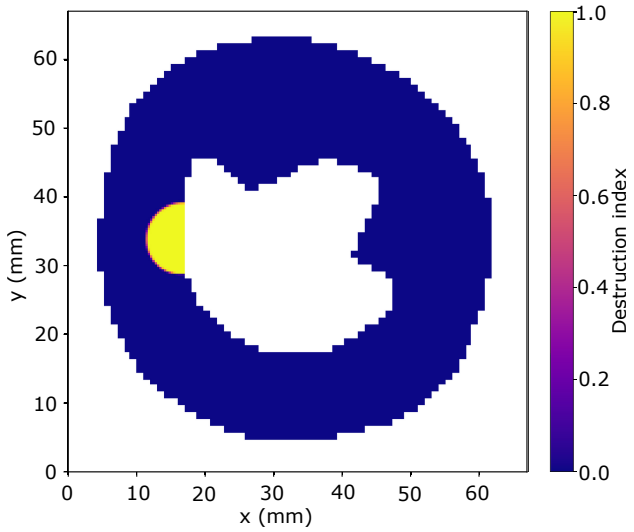

Figure 2. Mean tissue damage at the end of the simulation ($t = 340s$), based on $1,000$ Monte Carlo simulations.

Table 1. Model parameters for the simulation, with $T_l = 0°\text{C}$ and $T_s = -10°\text{C}$ defining the phase-change limits, basal metabolic heat generation $Q_{m0} = 684\ \text{W m}^{-3}$, and blood specific heat $c_{b0} = 3600\ \text{J (kg°C)}^{-1}$.

Parameter	Temperature	Value
κ	$T_l < T$	0.537
$[W/m°C]$	$T_s \leq T \leq T_l$	$0.537 + \frac{1.8-0.537}{T_s - T_l}(T - T_l)$
	$T < T_s$	1.8
Q_m	$T_l < T$	$Q_{m0}\, 3^{\frac{T-37}{10}}$
$[W/m^3]$	$T_s \leq T \leq T_l$	$Q_m(T_l)\dfrac{T - T_s}{T_l - T_s}$
	$T < T_s$	0
ρC	$T_l < T$	3641113
$[J/(m^3°C)]$	$T_s \leq T \leq T_l$	$\dfrac{\Delta H}{T_l - T_s} + \dfrac{(\rho C)_l + (\rho C)_s}{2}$
	$T < T_s$	1657800
ω_b	$T > T_s$	0.01
$[s^{-1}]$	$T \leq T_s$	0
$\rho_b C_b$	$T > T_s$	$c_{b0}\left(\dfrac{T - T_s}{37 - T_s}\right)^2$
$[J/(m^3°C)]$	$T \leq T_s$	0

new probe temperature is calculated by applying a linear cooling rate of approximately $-10.54°C/s$ to the previous temperature. Additionally, a lower limit is enforced to ensure that the probe temperature does not drop below $-100°C$.

3.3. Experiments

To perform uncertainty quantification, we conduct 1,000 simulations using the Monte Carlo method, with the thawing duration parameter treated as a random variable. We store the quantities of interest for each experiment, including the number of damaged cells at each time step and the history of the damaged area.

Figure 2 depicts the average damage distribution at the last time step across all simulations. The mean and standard deviation for the evolution of the injured area over time are shown in Figure 3A. Finally, Figure 3B illustrates the progression of the damaged region by showing the minimum and maximum distances from the probe to the damage front along with their standard deviation.

4. Discussions

The results demonstrate the spatial distribution of tissue injury and its progression during cryoablation. Figure 2 shows that damage is concentrated around the cryoprobe with a smooth radial decay, reflecting thermal gradients and perfusion. In Figure 3A, the injured area grows rapidly at the beginning of the freezing phase and then stabilizes, while the variability across simulations highlights the influence of thawing duration. Figure 3B shows the progression of the damage front through minimum and maximum distances from the probe, with the associated variability indicating irregular lesion geometry. These findings underscore the importance of incorporating uncertainty quantification to predict lesion formation better and optimize cryoablation protocols.

5. Conclusions and Future Works

The presented framework enables the evaluation of the effects of different parameters on the outcome of cardiac cryosurgery. The experiments demonstrated that the in-

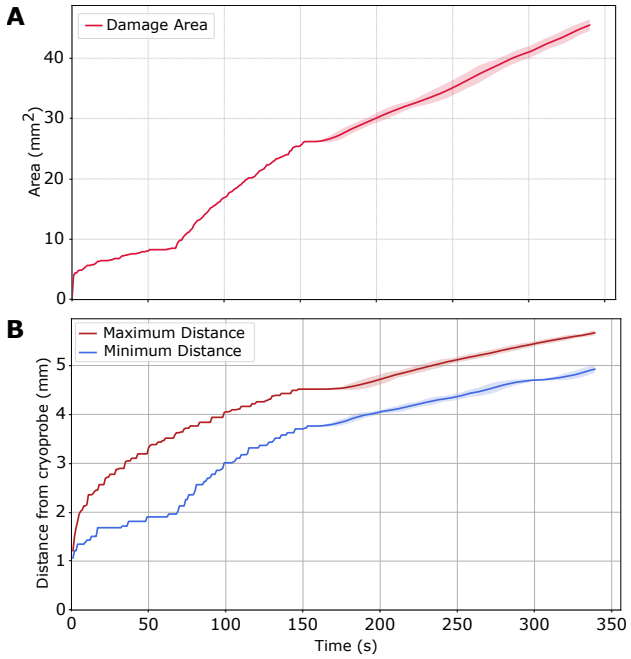

Figure 3. (A) Evolution of total damaged area over time; (B) minimum and maximum distances from the probe center to the damage boundaries. Solid lines indicate the mean and shaded regions the standard deviation from $1,000$ Monte Carlo simulations.

terim thawing duration influences the extent of myocardial damage after the cardiac cryoablation. This study demonstrates that this computational framework can be a valuable tool for *in silico* trials that optimize parameters to achieve improved clinical results.

For future work, we plan to analyze different types of protocols employed in cardiac cryoablation, utilizing patient-specific geometries, to propose an optimized protocol tailored to a specific patient.

Acknowledgements

The authors thank Minas Gerais State Research Support Foundation (FAPEMIG) - PCE-00048-25 APQ-01226-21, APQ-02513-22; FINEP (SOS Equipamentos 2021 AV02 0062/22); "Coordenação de Aperfeiçoamento de Emprego de Nível Superior" (CAPES), the Tutorial Education Group of Computational Engineering (GET-EngComp), and the Universidade Federal de Juiz de Fora (UFJF) for funding this work.

References

[1] Kornej J, Börschel CS, Benjamin EJ, Schnabel RB. Epidemiology of atrial fibrillation in the 21st century: Novel methods and new insights. Circulation Research June 2020; 127(1):4–20. ISSN 1524-4571.

[2] Handler M, Fischer G, Seger M, Kienast R, Hanser F, Baumgartner C. Simulation and evaluation of freeze-thaw cryoablation scenarios for the treatment of cardiac arrhythmias. BioMedical Engineering OnLine February 2015; 14(1). ISSN 1475-925X.

[3] Hosseini SM, Rozen G, Saleh A, Vaid J, Biton Y, Moazzami K, Heist EK, Mansour MC, Kaadan MI, Vangel M, Ruskin JN. Catheter ablation for cardiac arrhythmias. JACC Clinical Electrophysiology November 2017;3(11):1240–1248. ISSN 2405-500X.

[4] Andrade JG, Rivard L, Macle L. The past, the present, and the future of cardiac arrhythmia ablation. Canadian Journal of Cardiology December 2014;30(12):S431–S441. ISSN 0828-282X.

[5] González-Suárez A, Pérez JJ, Irastorza RM, D'Avila A, Berjano E. Computer modeling of radiofrequency cardiac ablation: 30 years of bioengineering research. Computer Methods and Programs in Biomedicine February 2022; 214:106546. ISSN 0169-2607.

[6] Hachem AH, Marine JE, Tahboub HA, Kamdar S, Kanjwal S, Soni R, Kanjwal K. Radiofrequency ablation versus cryoablation in the treatment of paroxysmal atrial fibrillation: A meta-analysis. Cardiology Research and Practice 2018;2018:1–10. ISSN 2090-0597.

[7] Wit AL, Rosen MR. Pathophysiologic mechanisms of cardiac arrhythmias. American Heart Journal October 1983; 106(4):798–811. ISSN 0002-8703.

[8] Wu Z, Liu Y, Tong L, Dong D, Deng D, Xia L. Current progress of computational modeling for guiding clinical atrial fibrillation ablation. Journal of Zhejiang University SCIENCE B October 2021;22(10):805–817. ISSN 1862-1783.

[9] Handler M, Fischer G, Seger M, Kienast R, Nowak CN, Pehböck D, Hintringer F, Baumgartner C. Computer simulation of cardiac cryoablation: Comparison with in vivo data. Medical Engineering amp Physics December 2013; 35(12):1754–1761. ISSN 1350-4533.

[10] Tanwar S, Famhawite L, Verma PR. Numerical simulation of bio-heat transfer for cryoablation of regularly shaped tumours in liver tissue using multiprobes. Journal of Thermal Biology April 2023;113:103531. ISSN 0306-4565.

[11] LeVeque RJ. Finite difference methods for ordinary and partial differential equations: steady-state and time-dependent problems. SIAM, 2007.

[12] Reis RF, dos Santos Loureiro F, Lobosco M. 3D numerical simulations on gpus of hyperthermia with nanoparticles by a nonlinear bioheat model. Journal of Computational and Applied Mathematics 2016;295:35–47.

Address for correspondence:

Ruy Freitas Reis
Universidade Federal de Juiz de Fora/Departamento de Ciência da Computação, Room 429
ruy.reis@ufjf.br